Applied Catalysis B: Environmental 126 (2012) 108–120

Contents lists available at SciVerse ScienceDirect

Applied Catalysis B: Environmental

journal homepage: www.elsevier.com/locate/apcatb

Insights into the effect of surface hydroxyls on CO_2 hydrogenation over Pd/γ-Al_2O_3 catalyst: A computational study

Riguang Zhang, Hongyan Liu, Baojun Wang*, Lixia Ling

Key Laboratory of Coal Science and Technology of Ministry of Education and Shanxi Province, Taiyuan University of Technology, Taiyuan 030024, Shanxi, People's Republic of China

ARTICLE INFO

Article history:
Received 18 February 2012
Received in revised form 8 July 2012
Accepted 16 July 2012
Available online 23 July 2012

Keywords:
Pd/γ-Al_2O_3
CO_2 hydrogenation
Hydroxylation
Support
Density functional theory

ABSTRACT

The elementary steps leading to the formation of HCOO and CO via CO_2 hydrogenation, two important intermediates contributing to methanol and methane formation, respectively, have been explored to identify hydroxylation effect of the oxide support on the selectivity in CO_2 hydrogenation on Pd/γ-Al_2O_3 catalyst by the density functional theory together with slab model calculations. Two models: tetramer Pd4 cluster supported on the dry γ-Al_2O_3(1 1 0) surface, D(Pd4), and on the hydroxylated γ-Al_2O_3(1 1 0) surface, H(Pd4), have been employed to model Pd/γ-Al_2O_3 catalyst. Meanwhile, Pd(1 1 1) surface is used to model the unsupported large Pd particle sizes. On D(Pd4), the formation of CO is preferred both kinetically and thermodynamically. On H(Pd4), HCOO formation becomes more favorable kinetically while CO formation is more facile thermodynamically. However, Pd(1 1 1) surface has not shown strong selectivity and activity for CO_2 hydrogenation to HCOO or CO. These results show that varying the properties of γ-Al_2O_3 support can alter the selectivity of CO_2 hydrogenation, moreover, the presence and number of low-coordinated Pd particles is of great importance to improve the overall activity and selectivity of CO_2 hydrogenation. Our results also show that to achieve high selectivity of CO_2 hydrogenation, Pd/γ-Al_2O_3 catalyst has to get help from additives, which should be able to improve its dispersion or to control the hydroxylation. The present study provides the basis and one of the directions to the design of improved catalysts in CO_2 hydrogenation for methanol, methane and other products.

1. Introduction

Catalytic recycling of CO_2, the major man-made greenhouse gas, to more useful compounds is currently under consideration among the possible approaches for mitigating its emissions to the atmosphere [1–3]. In this regard, the selective hydrogenation of CO_2 to methanol or methane has emerged in the last decade as a promising and viable option [4–8], formate and CO are two important intermediates in the selective hydrogenation of CO_2, which have been proposed as precursors for the formation of final products methanol and methane, respectively. Evidence for the existence of the key intermediate formate species in CO_2 hydrogenation to methanol has been derived from both infrared (IR) [9] and temperature-programmed desorption (TPD) [10] spectra. On the other hand, CO is a product of reverse WGS reaction, and it has been suggested as the key intermediate for methane formation [11–15]. These studies suggest that the products of the initial CO_2 hydrogenation steps will determine the distribution of the final products.

Nowadays, Cu/ZnO-Al_2O_3 catalyst is typically used to synthesize methanol on an industrial scale from mixtures of $CO/CO_2/H_2$ (syngas) [3,16], and Ni-based catalysts have been widely chosen as an active methanation catalyst to dissociate CO in the presence of hydrogen and subsequently form methane [17–20]. However, these catalysts are easily susceptible to sulfur poisoning [21]. Therefore, a high potential of metal Pd has been employed as an active catalyst for the hydrogenation of carbon oxides (CO and CO_2) [22–29,4,30–40], and Pd-based catalysts have been reported to be more effective than the conventional Cu-based catalysts. For example, Fujitani et al. [28] prepared an active Pd/Ga_2O_3 catalyst for methanol synthesis from CO_2 hydrogenation, which can well compete with the classical Cu/ZnO catalyst. Later on, Shen et al. [29] reported that the catalytic activity of Pd/CeO_2 in methanol synthesis from CO and H_2 is significantly higher than that of Cu catalyst. Naito et al. [36,37] studied the CO hydrogenation over Pd/CeO_2 catalyst, suggesting that both methane and methanol can be formed on this catalyst. Importantly, Erdöhelyi and co-workers [34,35] investigated the hydrogenation of CO_2 over Pd supported by Al_2O_3, TiO_2, SiO_2 and MgO, respectively, in situ IR revealed that bonded CO and formate species were present on the catalyst surface during the reaction, and formate species was more easily formed. However, Vannice and Garten [38] reported that Pd/Al_2O_3 catalyst was an active and selective catalyst for methane, which was also supported

* Corresponding author at: No. 79 Yingze West Street, Taiyuan 030024, People's Republic of China. Tel.: +86 351 6018539; fax: +86 351 6041237.
E-mail addresses: wangbaojun@tyut.edu.cn, quantumtyut@126.com (B. Wang).

0926-3373/$ – see front matter © 2012 Elsevier B.V. All rights reserved.
http://dx.doi.org/10.1016/j.apcatb.2012.07.009

by Rothaemel et al.'s studies [39]. Thus, on the basis of above experimental facts, we can see that although there are some discrepancies for the activity and selectivity of Pd, Pd is found to be a good catalyst of CO_2 hydrogenation. As a result, developing catalysts for CO_2 hydrogenation efficiently and selectively has been one of the major challenges in catalysis.

On the other hand, among above oxide-supported Pd catalysts, Al_2O_3, γ-Al_2O_3 in particular, is widely used as support in heterogeneous catalysis including CO_2 conversion, since metal particles supported on oxides such as γ-Al_2O_3 have been shown to be effective for catalytic conversion of CO_2 [41–43], and a good dispersion of metal particles on γ-Al_2O_3 due to high porosity and specific surface area [44–47]. Moreover, the presences of both acidic and basic sites on γ-Al_2O_3 surface may affect the reaction of CO_2 participation [43]. However, for γ-Al_2O_3-supported metal catalysts, the surface of γ-Al_2O_3 support will inevitably be hydrated/hydroxylated under a realistic reaction environment; further, the nature of the surface will be modified [48–53]. This modification will lead to an effect on the active species-support interaction and further on the reactions taking place over the catalyst. For example, Lomot and Karpinski [51] studied the effect of pretreatment on the activity of Pd/γ-Al_2O_3 catalyst for the cyclopentane/deuterium exchange reaction, suggesting that an active γ-Al_2O_3-supported catalyst should have two types of sites: Lewis acid sites for cyclopentane binding and surface hydroxyls for proton transfer. Afterwards, Pan et al. [49] investigated the adsorption and activation of CO_2 over the dry and hydroxylated γ-Al_2O_3-supported metal dimmers, indicating that hydroxylation of the support surface weakens the binding of metal dimmers to the surface, and reduces the amount of charge transferred to CO_2, as well as weakens the CO_2 chemisorption bonds. Later on, Pan et al. [52] further studied the effect of surface hydroxyls on CO_2 hydrogenation over Ni/γ-Al_2O_3 catalyst, which showed that HCOO formation was preferred kinetically on the dry γ-Al_2O_3(1 1 0) surface, however, CO formation became more favorable both kinetically and thermodynamically on the hydroxylated surface, namely, the surface nature of the γ-Al_2O_3 support can adjust and alter the product distribution for the hydrogenation of CO_2. In addition, Valero et al. [54,55] have investigated the adsorption of Pd_n ($1 \le n \le 5$) clusters and Pd films on γ'-Al_2O_3 surfaces. These theoretical results already suggested the crucial role of hydroxylation on the stability and morphology properties of Pd clusters on γ'-Al_2O_3, an effect of hydroxylation that must be considered to study the reactivity of the supported clusters.

In order to better understand the role that hydroxylation of the γ-Al_2O_3 plays in CO_2 conversion on Pd/γ-Al_2O_3 catalyst and illustrate the key factors that affect the selectivity and activity of the catalysts, in the present work, we use a model catalyst, Pd/γ-Al_2O_3, to probe into the effect of hydroxylation of the γ-Al_2O_3 support on CO_2 hydrogenation. However, given the porosity and disorder of the γ-Al_2O_3 support, experimental characterization of alumina supported heterogeneous catalysts is rather difficult. Thus, density functional theory (DFT) calculations on realistic γ-Al_2O_3 model are mandatory to obtain relevant insight into heterogeneous catalysis [43,48]. Up to now, to our knowledge, few studies about the effect of hydroxylation of the γ-Al_2O_3 support on CO_2 hydrogenation over Pd/γ-Al_2O_3 catalyst have been reported. A detailed characterization of CO_2 hydrogenation over Pd/γ-Al_2O_3 catalyst at the molecular level will help us better understand the underlying mechanisms of the reactions and aid in the elucidation of key factors that affect the performance of the catalysts. Meanwhile, an atomic-scale understanding of the reaction mechanism would facilitate the design of improved catalysts for CO_2 hydrogenation.

Therefore, in this study, focusing on the atomic level detail of CO_2 hydrogenation-active species-support, we report a significant hydroxylation effect of the γ-Al_2O_3 support on CO_2 hydrogenation over Pd/γ-Al_2O_3 catalyst using the DFT slab calculations, in which the elementary steps leading to the formation of HCOO and CO have been systematically investigated toward CO_2 hydrogenation over the dry and hydroxylated γ-Al_2O_3-supported Pd catalysts, as well as Pd(1 1 1) surface, respectively. The main idea is to compare the potential energy profile of CO_2 hydrogenation among these three catalysts; we expect that the existence of surface hydroxyls on the γ-Al_2O_3 surface can be responsible for the observed CO_2 hydrogenation selectivity. This paper is organized as follows: computational details are described in Section 2. Results and discussion are given in Section 3. Finally, the conclusions are presented in Section 4.

2. Computational details

2.1. Computational models

The γ-Al_2O_3 structural models have been proposed based on the defective spinel model [56,57] and non-spinel model [48]. In this study, we employ the non-spinel model due to the fact that its (1 0 0) surface exposes the penta-Al sites that is observed experimentally [58,59]. The non-spinel γ-Al_2O_3 model has been employed to construct surfaces in the previous studies [60–62], thus, we use non-spinel γ-Al_2O_3 as previous studies to model the γ-Al_2O_3 surface in this study. Meanwhile, γ-Al_2O_3(1 1 0) surface is selected to model the support. This is based on the fact that the (1 1 0) surface is estimated to comprise 83% of the total surface area of γ-Al_2O_3, whereas the (1 0 0) surface is estimated to account for only 17% of the total surface area [48]. The (1 1 0) surface is modeled by a supercell with a dimension of $8.40 \times 8.07 \times 19.17$ Å. Twelve Al_2O_3 molecular units in the slab are distributed in six layers. The vacuum region separating the slabs in the direction perpendicular to the surface is set to 12 Å.

Then, 4-atom Pd (Pd4) cluster is constructed in both tetrahedral and planar configurations to model Pd catalyst supported on γ-Al_2O_3(1 1 0) surface. Our results show that the tetrahedral Pd4 cluster configuration is found to be more favorable energetically than the planar one in the gas phase, which is in agreement with the other studies [63,64]. Further, upon binding on the γ-Al_2O_3(1 1 0) surface, the interaction of the tetrahedral configuration is also much stronger than that of the planar configuration. Since the tetrahedral configuration is the smallest unit, which can provide a three-dimensional structure to probe both metal–metal and metal–support interactions. We therefore focus our attention on the tetrahedral configuration in this study, which is employed to explore its interaction with the supporting γ-Al_2O_3(1 1 0) surface.

As a result, taking the surface hydroxyls of the support γ-Al_2O_3 into consideration, two models: Pd4 cluster supported on the dry (fully dehydrated) γ-Al_2O_3(1 1 0) surface and on the partially hydroxylated γ-Al_2O_3(1 1 0) surface, have been constructed to model Pd/γ-Al_2O_3 catalyst. In all calculations, the bottom two layers of the γ-Al_2O_3(1 1 0) surface are frozen in their bulk positions, whereas the top four layers together with the Pd4 cluster and the species involved in CO_2 hydrogenation are allowed to relax.

2.2. Computational methods

All calculations are carried out in the framework of DFT using the Dmol^3 program package in Materials Studio 4.4 [65,66], where the generalized gradient approximation (GGA) corrected the exchange-correlation functional proposed by Perdew–Burke–Ernzerhof (PBE) [67] is chosen together with the double numerical basis set with polarization (DNP) [68]. The inner electrons of Pd and Al atoms are kept frozen and replaced by an

effective core potential (ECP) [69,70], and other atoms are treated with an all-electron basis set. Spin unrestricted is performed. Brillouin-zone integrations have been performed using medium k-point grid. Meanwhile, in order to determine accurate activation barrier of the reaction, we chose complete LST/QST approach to search for transition states of the reaction [71]. In addition, frequency analysis has been used to validate the optimized transition state structures, and TS confirmation is performed on every transition state to confirm that they lead to the desired reactants and products.

The binding energy of Pd4 cluster with the γ-Al_2O_3 surface, E_{bind}, is calculated as follows:

$$E_{bind} = E(\gamma\text{-}Al_2O_3) + E(\text{Pd4 cluster}) - E\left(\frac{\text{Pd4 cluster}}{\gamma\text{-}Al_2O_3}\right)$$

where $E(\gamma\text{-}Al_2O_3)$, E(Pd4 cluster) and E(Pd4 cluster/γ-Al_2O_3) are the total energies of the bare γ-Al_2O_3 slab, the free Pd4 cluster, and γ-Al_2O_3 slab with Pd4 cluster, respectively.

The adsorption energy, E_{ads}, is defined as follows:

$$E_{ads} = E_{sub} + E_{mol} - E_{mol/sub}.$$

where $E_{mol/sub}$ is the total energy of adsorbate–substrate system in the equilibrium state, E_{sub} and E_{mol} are the total energies of substrate and free adsorbate alone, respectively. With this definition, more positive values reflect strong interaction of adsorbed species with surface atoms.

3. Results and discussion

3.1. The mechanisms of CO_2 hydrogenation on D(Pd4)

3.1.1. Pd4 cluster supported on the dry γ-Al_2O_3(1 1 0) surface

The side and top views of the dry γ-Al_2O_3(1 1 0) surface are provided in Fig. 1a to label the surface atoms. On this surface, 3-fold-coordinated Al (Al_{3c}), 4-fold-coordinated Al (Al_{4c}), 2-fold-coordinated O (O_{2c}) and 3-fold-coordinated O (O_{3c}) atoms are exposed, among which Al_{3c}, Al_{4c} and O_{2c} are coordinately unsaturated. Then, different surface sites are explored for the interaction of Pd4 cluster with the dry γ-Al_2O_3(1 1 0) surface, and adsorption at these sites results in a number of configurations. The most stable adsorption configuration of Pd4 cluster among the stable sites is selected as the substrate in the study of CO_2 hydrogenation and is denoted as D(Pd4), with D indicating the dry oxide surface. The structure of D(Pd4) with key structural parameters is shown in Fig. 1b.

In D(Pd4), three Pd atoms (Pd_1, Pd_2 and Pd_3) interact with the surface directly; forming two Pd_1—O_{2c} bonds (2.14 and 2.21 Å), one Pd_2—Al_{3c} bond (2.50 Å) and two Pd—Al_{4c} bonds (2.55 and 2.56 Å), Pd_4 atom is located at the top vertex away from the support

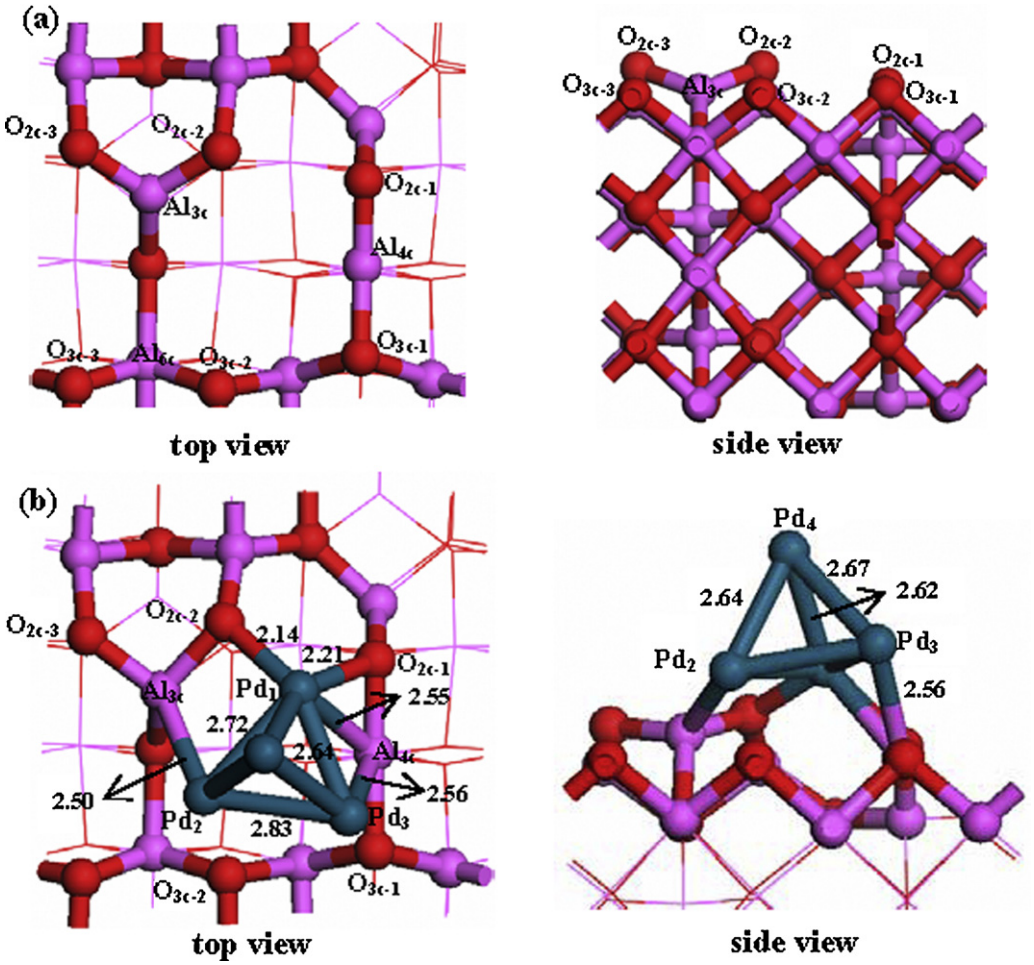

Fig. 1. The side and top views of (a) the dry γ-Al_2O_3(1 1 0) surface and (b) Pd4 cluster supported on the dry surface, D(Pd4), respectively. Bond lengths are in Å. Pink balls stand for Al atoms, red balls stand for O atoms, and blue balls stand for Pd atoms. (For interpretation of the references to color in this figure legend, the reader is referred to the web version of the article.)

surface. The binding energy of the supported Pd4 cluster in D(Pd4) is 406.4 kJ mol^{-1}.

3.1.2. Single and coadsorbed configuration of CO_2 and H on D(Pd4)

Previous experimental and theoretical studies have investigated the interaction of hydrogen molecule with Pd metal surfaces [72–75], suggesting that hydrogen mainly exists in the form of atomic hydrogen on metal Pd. Meanwhile, in hydrogenation conditions, the Pd4 clusters will probably contain a higher concentration of hydrogen atoms. However, since our aim in this study is to examine the effect of surface hydroxyls on CO_2 hydrogenation, for the sake of simplicity, only the interaction of CO_2 with one atomic H for CO_2 hydrogenation over Pd/γ-Al_2O_3 catalyst is investigated. The impact of H-coverage will be examined in our next work. Therefore, the structures of CO_2 molecule and H adatom separately adsorbed on D(Pd4) are first investigated, and the most stable adsorption configurations of CO_2 and H separately adsorbed on D(Pd4) with key structural parameters are provided in Supplementary materials.

Then, the coadsorbed CO_2 and H on D(Pd4) is examined. The most stable configuration for the coadsorbed CO_2 and H on D(Pd4) is presented in Fig. 2, and is named as D(R). In D(R), CO_2 still interacts with Pd_4 atom via C—Pd_4 (2.11 Å) bond. The lengths of C—O_a and C—O_b bonds are 1.21 and 1.23 Å, respectively, and the angle of O_a—C—O_b is 150.1°. Moreover, H still binds Pd_4 and Pd_3 atoms, and the H—Pd_4 and H—Pd_3 bonds are 1.76 and 1.65 Å, respectively. The adsorption energy for the coadsorbed CO_2 and H on D(Pd4) is 321.0 kJ mol^{-1}. D(R) serves as the starting configuration for CO_2 hydrogenation to HCOO or to CO on D(Pd4). In the following section, for clarity, the intermediates, transition states and products involved in the pathways of CO_2 hydrogenation on D(Pd4) are prefixed with D.

3.1.3. CO_2 hydrogenation to HCOO on D(Pd4)

The pathway for HCOO formation starts from D(R), as shown in Fig. 2. The potential energy profile for the pathway from D(R) to D(HCOO) is presented in Fig. 3 as a black line. The structures of all the intermediates, transition states and products involved in this pathway are shown along with the potential energy profile.

Beginning with D(R), adsorbed CO_2 first goes away from the Pd4 cluster via a transition state D(TS1), leading to the formation of D(IM1) intermediate. In D(IM1), the geometrical structure of CO_2 are closed to that in gas phase free molecule, the lengths of C—O_a and C—O_b bonds are 1.17 and 1.18 Å, respectively. The distance between H atom and C atom of CO_2 is 3.44 Å. This step is slightly endothermic by 2.1 kJ mol^{-1}, with a small activation barrier of 13.2 kJ mol^{-1}. Subsequently, with H adatom approaching the C atom of CO_2, H adatom is transferred from the Pd_3—Pd_4 bridge to the C atom through the transition state D(TS2). In D(TS2), adsorbed CO_2 interacts with Pd_4 atom through O_b atom, and the distance between H and C decreases to 1.89 Å from 3.44 Å in D(IM1). The angle of CO_2 is 152.1°, two C—O bond lengths are 1.20 and 1.22 Å, respectively. This step breaks two H—Pd bonds and forms a C—H bond (1.12 Å) and Pd_4—O_b bond (2.03 Å) in D(IM2). In D(IM2), HCOO is adsorbed over the substrate in monodentate form. This elementary reaction has a very large activation barrier of 242.5 kJ mol^{-1}, and the reaction is endothermic by 82.4 kJ mol^{-1}. Finally, the monodentate HCOO species in D(IM2) can convert into a more stable and bidentately bound HCOO species in D(HCOO) via the transition state D(TS3), this step is exothermic by 55.7 kJ mol^{-1}, with an activation barrier of 53.6 kJ mol^{-1}. In D(HCOO), the HCOO species binds the substrate through the O_a—Pd_2 (2.11 Å) and O_b—Pd_4 (2.17 Å) bonds, as shown in Fig. 3. The C—O_a and C—O_b bonds are 1.28 and 1.26 Å, respectively, and the O_a—C—O_b angle is 129.3°. These structural parameters are in agreement with those observed in HCOO adsorption on Pd surfaces [76,77].

3.1.4. CO_2 hydrogenation to CO on D(Pd4)

Starting from D(R), the reaction product of CO formation is the coadsorbed CO and OH, denoted as D(CO + OH). The potential energy profile from D(R) to D(CO + OH) is also shown in Fig. 3 as a red line. The structures of all species involved in this process are also presented together with the potential energy profile.

This pathway first starts from the migration of H adatom from the Pd_3—Pd_4 bridge site in D(R) to the Pd_2—Pd_4 bridge site in D(IM3) via a transition state D(TS4). This step forms a Pd—O_b bond in D(IM3), in which both C and O_b atoms of CO_2 link with one Pd_4 atom. In D(IM3), the C—Pd_4 and O_b—Pd_4 bonds are 2.29 and 2.29 Å, respectively. Two C—O bond lengths are 1.19 and 1.21 Å, respectively. The O_a—C—O_b angle is 159.1°, and the distance between H and O_a is 3.27 Å. The activation barrier for this elementary reaction is 76.8 kJ mol^{-1}, and the reaction is endothermic by 17.3 kJ mol^{-1}. Then, when H adatom approaches the O_a atom of adsorbed CO_2 molecule, H adatom is transferred from the Pd_2—Pd_4 bridge to the O_a atom of CO_2 through the transition state D(TS5), which leads to a trans-carboxyl (*trans*-COOH) species in D(IM4). This step breaks two H—Pd bonds and forms an O_a—H bond (1.00 Å) in D(IM4). In D(TS5), the distance between H and O_a decreases

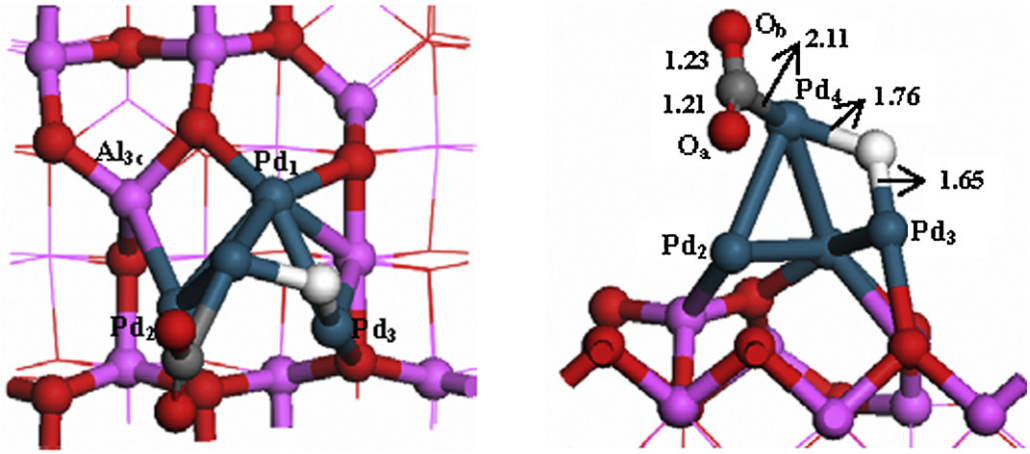

Fig. 2. The stable configuration D(R) of the co-adsorbed CO_2 and H on D(Pd4). Bond lengths are in Å. Grey balls stand for C atoms, white balls stand for H atoms, and others are the same as in Fig. 1. (For interpretation of the references to color in this figure legend, the reader is referred to the web version of the article.)

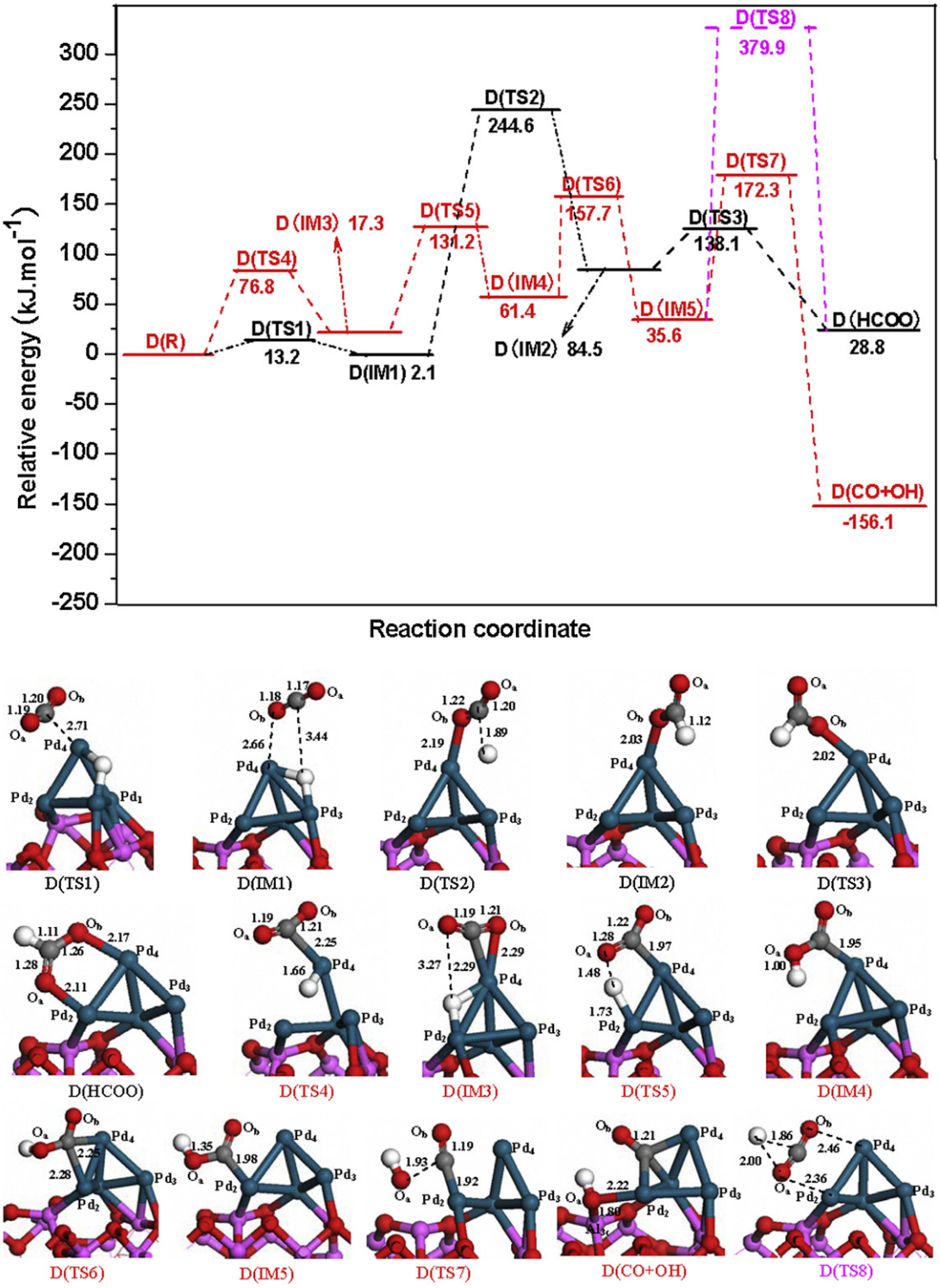

Fig. 3. Potential energy profiles for CO_2 hydrogenation to HCOO (black line) and to CO (red line) on D(Pd4). Structures of the intermediates, transition states and products are also shown. Bond lengths are in Å. See Figs. 1 and 2 for color coding. (For interpretation of the references to color in this figure legend, the reader is referred to the web version of the article.)

to 1.48 Å from 3.27 Å in D(IM4), the angle of CO_2 is 143.2°, two C—O bond lengths are 1.28 and 1.22 Å, respectively. The Pd_2—H and Pd_4—C bond lengths are 1.73 and 1.97 Å, respectively. This step is endothermic by 44.1 kJ mol^{-1}, with a high activation barrier of 113.9 kJ mol^{-1}. The third step corresponds to the isomerization from *trans*-COOH species in D(IM4) to *cis*-COOH species in D(IM5) via a transition state D(TS6). In this step, COOH transfer from Pd_4 atom in D(IM4) to Pd_2 atom in D(IM5). In D(TS6), COOH is located at Pd_2—Pd_4 bridge site, and the lengths of C—Pd_4 and C—Pd_2 bonds are 2.25 and 2.28 Å, respectively. This *trans-cis*-isomerization step is found to be exothermic by 25.8 kJ mol^{-1}, and the activation barrier is 96.3 kJ mol^{-1}. In the last step, the *cis*-COOH species in D(IM5) dissociates into the coadsorbed CO and OH group in D(CO + OH) through transition state D(TS7). In D(TS7), the C—O_a bond breaks, the distance between C and O_a increases to 1.93 Å from 1.35 Å in D(IM5), and the C—O_b bond length is 1.19 Å. This step is largely

exothermic, by 191.7 kJ mol^{-1}, and has a significantly high activation barrier of 136.7 kJ mol^{-1}. In D(CO + OH), the OH group binds the substrate through a newly formed Pd_2—O_a (2.22 Å) and Al_{3c}—O_a (1.80 Å) bonds, while CO binds the three-fold site of the Pd cluster through three Pd—C bonds, and the C—O_b bond length of CO is 1.21 Å, indicating that the C—O_b bond is activated in comparison with that of the free CO molecule (1.14 Å), and the activation of C—O_b bond is in favor of the subsequent reaction.

In addition, among the possible reaction pathways, we investigate the isomerization from *cis*-COOH species in D(IM5) to HCOO species in D(HCOO) via a transition state D(TS8), this elementary step goes through hydrogen transfer from O_a atom in D(IM5) to C atom in D(HCOO). This step is slightly exothermic by 6.8 kJ mol^{-1}, with a very high activation barrier of 344.3 kJ mol^{-1}, as shown in Fig. 3 using a pink line. This result suggests that the isomerization reaction of *cis*-COOH into HCOO cannot compete with the dissociation reaction of *cis*-COOH into the coadsorbed CO and OH.

3.1.5. Brief summary

Above results show that the rate-determining step for HCOO formation is hydrogen transfer from supported Pd cluster to C atom of CO_2, and the dissociation of COOH into the coadsorbed CO and OH group is the rate-determining step for CO formation. Further, we can see from Fig. 3 that the highest barrier and reaction energy for the conversion of CO_2 to HCOO with D(R) are 244.6 and 28.8 kJ mol^{-1}, respectively, whereas those for CO formation are 157.7 and −156.1 kJ mol^{-1}, respectively. Consequently, the formation of CO becomes more favorable both kinetically and thermodynamically on D(Pd4). Furthermore, the migration of H adatom from the supported Pd4 cluster to adsorbed CO_2 is an essential step for CO_2 hydrogenation to HCOO or CO on D(Pd4).

3.2. The mechanism of CO_2 hydrogenation on H(Pd4)

3.2.1. Pd4 cluster supported on the hydroxylated γ-Al_2O_3(1 1 0) surface

As demonstrated by Digne et al. [48], the (1 1 0) surface will inevitably be hydrated/hydroxylated under a realistic reaction condition. Thus, following the study of CO_2 hydrogenation over D(Pd4) catalyst, we choose the partially hydroxylated γ-Al_2O_3(1 1 0) surface to characterize the effect of surface hydroxylation on the Pd4 cluster interaction with the surface and CO_2 hydrogenation. Our aim in the present work is to gain insight into the qualitative influence of γ-Al_2O_3 surface hydroxylation on CO_2 hydrogenation, not to describe a specific hydroxyl coverage, which could vary under given experimental conditions. As a result, in this study, only one H_2O molecule are considered for the hydroxylated γ-Al_2O_3(1 1 0) surface, the side and top views of this partially hydroxylated γ-Al_2O_3(1 1 0) surface are shown in Fig. 4a. In this surface unit cell, one H_2O molecule dissociates into a hydroxyl (O_wH_a) with the bond length of 0.97 Å, which occupies the Al_{3c} site through an O_w—Al_{3c}

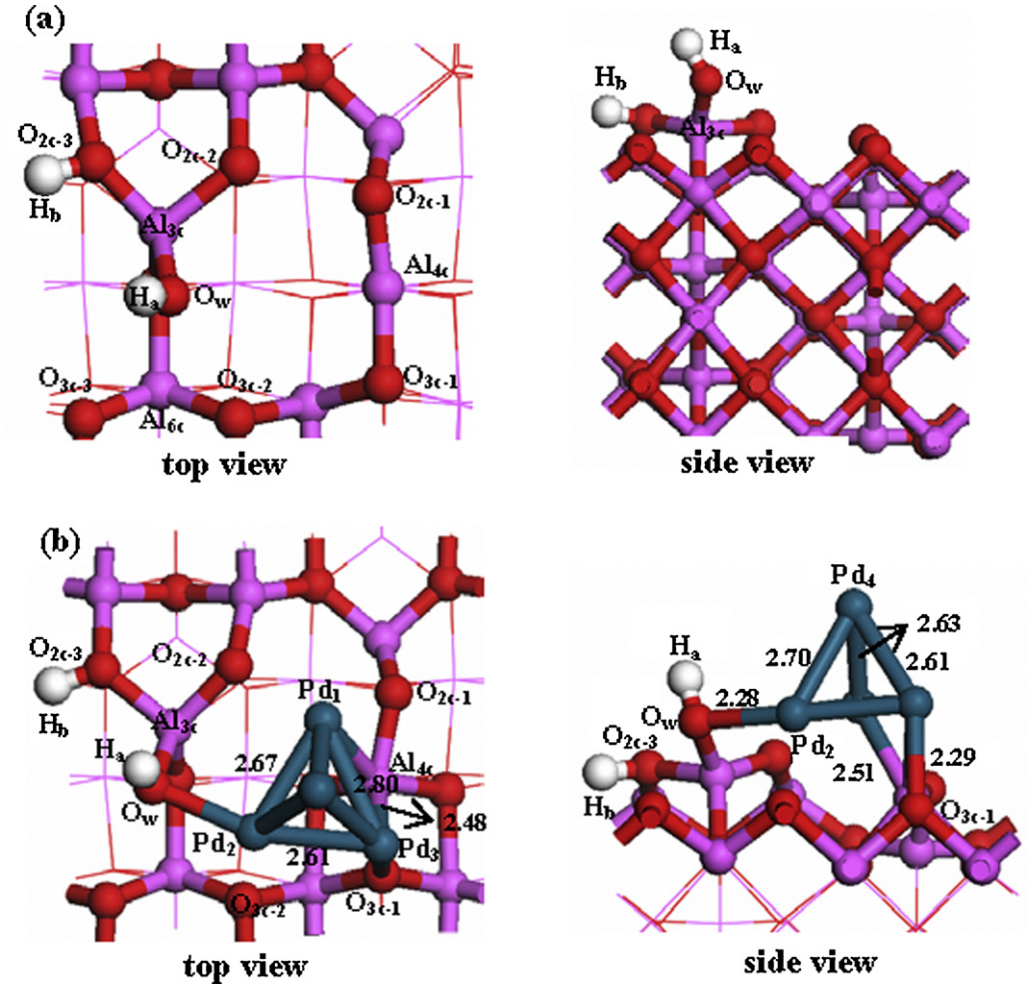

Fig. 4. The side and top views of (a) the hydroxylated γ-Al_2O_3(1 1 0) surface and (b) Pd4 cluster supported on the hydroxylated surface, H(Pd4), respectively. Bond lengths are in Å. See Figs. 1 and 2 for color coding. (For interpretation of the references to color in this figure legend, the reader is referred to the web version of the article.)

bond (1.77 Å). Meanwhile, a proton (H_b) binds with a neighboring $O_{2c\text{-}3}$ site through the H_b—$O_{2c\text{-}3}$ bond (0.90 Å). Therefore, there are two hydroxyls produced in each surface unit cell.

Again we explored a number of surface sites for Pd4 cluster supported on the hydroxylated surface. The most stable configuration is named as H(Pd4), with H indicating the partially hydroxylated surface. The structure of H(Pd4) with key structural parameters is shown in Fig. 4b. In H(Pd4), Pd4 cluster still interacts with the surface through three Pd atoms (Pd_1, Pd_2 and Pd_3), which forms two Pd—Al_{4c} bonds (2.51 and 2.48 Å), one Pd_3—O_{3c} bonds (2.29 Å) and one O_w—Pd_2 bond (2.28 Å), Pd_4 atom is still located at the top vertex away from the support surface. Therefore, H(Pd4) is selected as the substrate for CO_2 hydrogenation on the hydroxylated γ-Al_2O_3(1 1 0) surface. In addition, our results show that the binding energy of Pd4 cluster in H(Pd4) is 323.0 kJ mol^{-1}, which are 83.4 kJ mol^{-1} lower than those in D(Pd4). The decreased binding energy and charge transfer suggest that the presence of the hydroxyls on the surface can weaken the binding of Pd4 cluster to the support surface, and destabilize the Pd/γ-Al_2O_3 catalyst, which means that surface hydroxyls should be controlled in a reasonable range in order to keep catalyst stability.

3.2.2. Single and coadsorbed configuration of CO_2 and H on H(Pd4)

Similarly, the adsorptions of CO_2 and H on H(Pd4) individually are also investigated in order to probe the CO_2 hydrogenation pathways. In the following section, we use H_c to distinguish the H adatom from H_a and H_b on the hydroxylated γ-Al_2O_3(1 1 0) surface. The most stable configurations of CO_2 and H separately on H(Pd4) are provided in Supplementary materials. On the basis of the individual adsorption of CO_2 and H_c on H(Pd4), the coadsorbed CO_2 and H_c on H(Pd4) is further examined. The most stable configuration for the coadsorbed of CO_2 and H_c on H(Pd4) is presented in Fig. 5 and is denoted as H(R). In H(R), CO_2 interacts with the substrate through the C—Pd_4 (2.09 Å) and O_b—Pd_4 (2.29 Å) bonds. The lengths of C—O_a and C—O_b bonds are 1.20 and 1.24 Å, respectively, and the angle of O_a—C—O_b is 149.4°. Meanwhile, H_c is still located at a three-fold site through three H—Pd bonds (1.76, 1.79 and 1.80 Å). The distance between H_c and C is 3.33 Å, and the distance between H_c and O_a is 3.77 Å. The adsorption energy for the coadsorbed CO_2 and H_c on H(Pd4) is 323.1 kJ mol^{-1}. H(R) is selected as the starting configuration for CO_2 hydrogenation to HCOO or to CO on H(Pd4), and all the intermediates, transition states and products formed on H(Pd4) are prefixed with H to distinguish them from those on D(Pd4).

3.2.3. CO_2 hydrogenation to HCOO on H(Pd4)

H(R) serves as the reactant; the formation of HCOO is first discussed. Two possible pathways for CO_2 hydrogenation to HCOO on H(Pd4) have been considered, one is that H_c adatom attacks the C atom of CO_2 leading to HCOO, and the other is that H_a atom of O_wH_a attacks the C atom of CO_2 to form HCOO. Our results show that the latter pathway is far less favorable than the former pathway; the corresponding details of the less favorable pathway will be presented in Supplementary materials. Therefore, in the following section, only the most favorable pathway of H_c adatom attacking the C atom of CO_2 to form HCOO is discussed in the main text to compare with CO formation pathway, as shown using a red line in Fig. 6. The corresponding species involved in this process are again shown on the potential energy diagram.

The formation of H(HCOO) begins with the formation of an intermediate, H(IM1), through a transition state, H(TS1). In H(IM1), HCOO has been formed and adsorbed in monodentate form through the Pd_4—O_b bond (2.04 Å). In H(TS1), H_c only binds the Pd_4 atom with the H_c—Pd_4 bond length of 1.73 Å, suggesting that H_c adatom is transferred from a three-fold site in H(R) to the top site Pd_4 atom. The adsorbed CO_2 interacts with the substrate through Pd_4—O_b bond (2.29 Å), and the Pd_4—C bond in H(R) breaks. The angle of O_a—C—O_b is 136.2°, the lengths of two C—O bonds are 1.22 and 1.25 Å, respectively. The distance between H_c and C decreases to 1.44 Å from 3.33 Å in H(R). This step breaks two H—Pd bonds, and forms a C—H bond (1.12 Å) in H(IM1). The conversion from H(R) to H(IM1) is endothermic, by 85.3 kJ mol^{-1}, with a significant activation barrier of 143.4 kJ mol^{-1}. Then, similar to the third step in the HCOO pathway on D(Pd4), the monodentate HCOO species in H(IM1) relaxes into a more stable and bidentately bound HCOO species in H(HCOO) via a transition state H(TS2). The reaction energy and the activation barrier for this step are −54.1 kJ mol^{-1} and 23.5 kJ mol^{-1}, respectively. In H(HCOO), the HCOO species binds the substrate through the O_a – Pd_3 (2.30 Å) and O_b—Pd_4 (2.13 Å) bonds. The angle of O_a—C—O_b is 129.3°, and the lengths of C—O_a and C—O_b bonds are 1.26 and 1.28 Å, respectively. These structural properties are still similar to those on D(Pd4), as well as those observed in HCOO adsorption on Pd surfaces [76,77].

3.2.4. CO_2 hydrogenation to CO on H(Pd4)

Similar to the formation of HCOO, the formation of CO from the coadsorbed CO_2 and H_c on H(Pd4) also has two possible pathways, one is that H_c adatom attacking at the O_a atom of CO_2, the other is that H_a atom attacking at the O_a atom of CO_2. However, our calculated results show that the latter pathway does not exist,

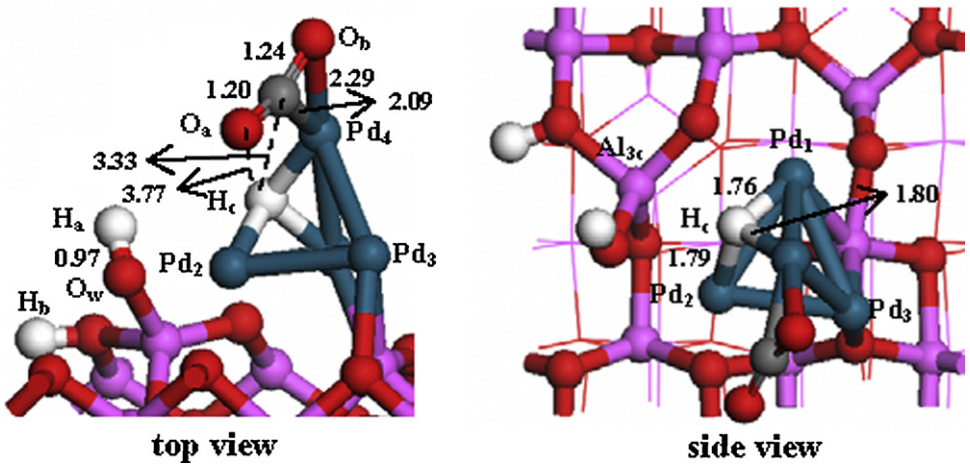

Fig. 5. The side and top views for the stable configuration H(R) of the coadsorbed CO_2 and H on H(Pd4). Bond lengths are in Å. See Figs. 1 and 2 for color coding. (For interpretation of the references to color in this figure legend, the reader is referred to the web version of the article.)

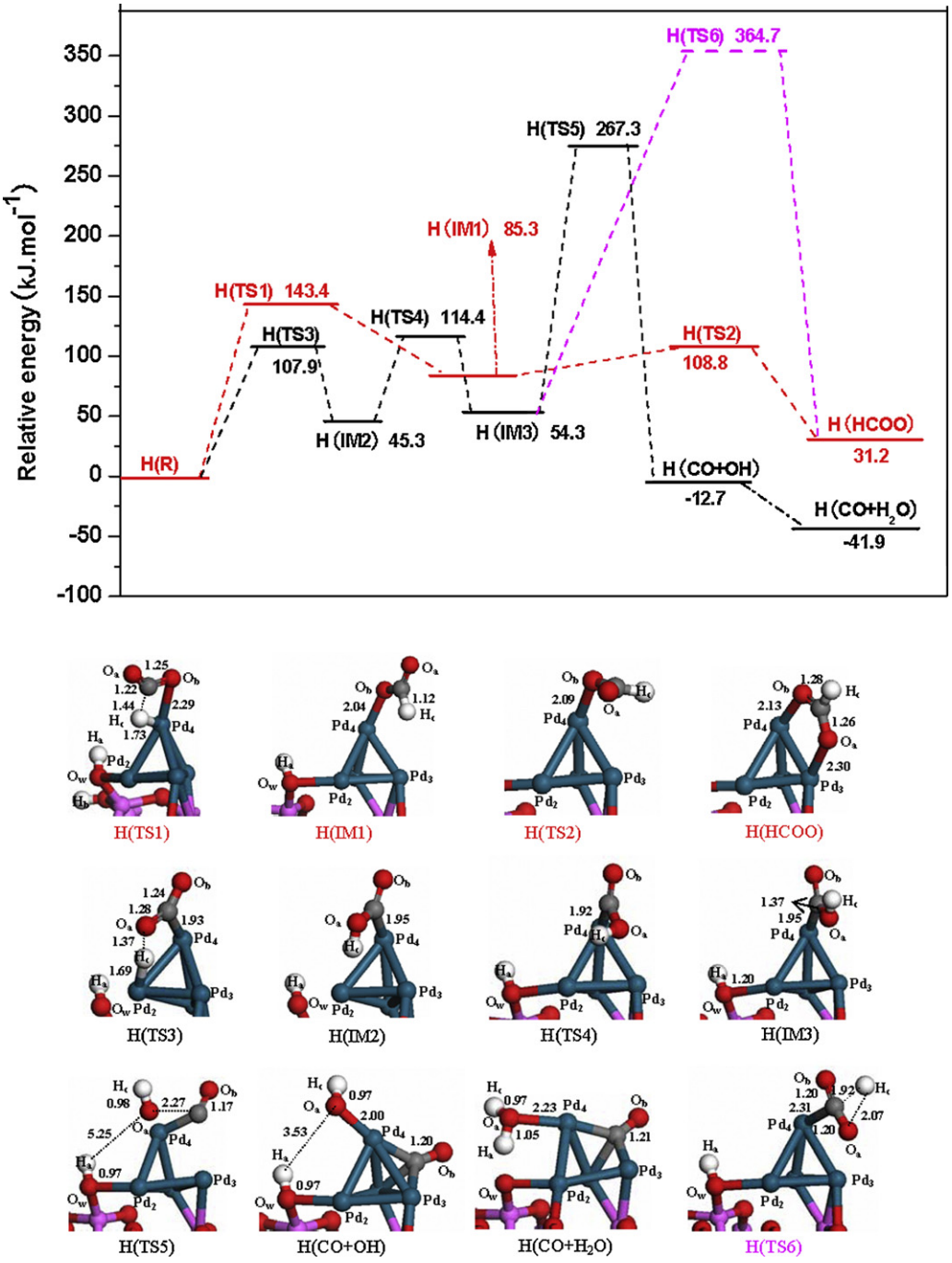

Fig. 6. Potential energy profiles of the most favorable pathway for CO_2 hydrogenation to HCOO (red line) and to CO (black line) on H(Pd4). Structures of the intermediates, transition states and products are also shown together with the potential energy profiles. Bond lengths are in Å. See Figs. 1 and 2 for color coding. (For interpretation of the references to color in this figure legend, the reader is referred to the web version of the article.)

because the optimized structure of $COOH_c$ adsorbed on H(Pd4) is always converted into adsorbed CO_2 and H_c binding the O atom over the support surface. Therefore, only the former pathway is discussed in this section, and the potential energy profile from H(R) to H(CO + H_2O) is shown using a black line in Fig. 6. Three intermediates, H(IM2), H(IM3) and H(CO + OH), and three transition states, H(TS3), H(TS4) and H(TS5) are involved in this process for HCOO formation, and the corresponding structures are also shown on the potential energy diagram.

The formation of CO first begins with the migration of H_c adatom from the three-fold site in H(R) to the O_a atom of CO_2 in H(IM2) via a transition state H(TS3). In H(TS3), H_c atom binds the substrate via Pd_2—H_c bond (1.69 Å), and the distance between H_c and O_a is shorten to 1.37 Å from 3.77 Å in H(R). The angle of O_a—C—O_b is 138.0°, and the C—O_a and C—O_b bond lengths are 1.28 and 1.24 Å, respectively. H(IM2) is the *trans*-carboxyl (*trans*-COOH) species, which interacts with the substrate through the Pd_4—C bond (1.95 Å). This step is endothermic by 45.3 kJ mol^{-1}, with an activation barrier of 107.9 kJ mol^{-1}. In the second step, the *trans*-carboxyl (*trans*-COOH) species in H(IM2) can isomerize to the *cis*-carboxyl (*cis*-COOH) species in H(IM3) through transition state H(TS4). In H(IM3), the *cis*-COOH binds the substrate through the Pd_4—C bond (1.95 Å), and the length of O_a—C bond is 1.37 Å. The reaction energy and activation barrier for this *trans*-*cis*-isomerization

step are 9.0 kJ mol^{-1} and 69.1 kJ mol^{-1}, respectively. The third step corresponds to the dissociation of *cis*-COOH in H(IM3) into the coadsorbed CO and OH groups in H(CO + OH) through the transition state H(TS5). In H(TS5), the distance between C and O_a increases to 2.27 Å from 1.37 Å in D(IM5), suggesting that the C—O_a bond breaks, and the C—O_b bond length is 1.17 Å. In H(CO + OH), the O_aH_c (0.97 Å) group binds the substrate through a newly formed Pd_4—O_a bond (2.00 Å), while CO_b binds at the three-fold site of Pd cluster through three Pd—C bonds, and the C—O_b bond length is 1.20 Å. This step is exothermic, by 67.0 kJ mol^{-1}, and has a very high activation barrier of 213.0 kJ mol^{-1}. Further, the O_aH_c group in H(CO + OH) combines with the proton (H_a) on the hydroxylated surface to form an adsorbed water molecule in H(CO + H_2O), all attempts to search for the transition state for the formation of H(CO + H_2O) from H(CO + OH) invariably show that the energy of the transition state is lower than that of the H(CO + H_2O), which confirm that H_a atom attacking the O_a atom of O_aH_c group can spontaneously produce the adsorbed water molecule. Thus, the last step is exothermic by 29.2 kJ mol^{-1}, without any activation barrier. In H(CO + H_2O), the H_2O molecule interacts with the substrate through the Pd_4—O_a bond (2.23 Å). Meanwhile, CO_b binds the three-fold site with the C—O_b bond length of 1.21 Å. Similar to the elongation of C—O_b bond in D(CO + OH), the activation of C—O_b bond can contribute to the subsequent reaction.

In addition, the isomerization from *cis*-COOH species in H(IM3) to HCOO species in H(HCOO) is also investigated. This elementary step goes through the migration of H_c atom from the O_a atom of *cis*-COOH species in H(IM3) to the C atom of HCOO species in H(HCOO) through transition state H(TS6). This step is exothermic by 23.1 kJ mol^{-1}, with the highest activation barrier of 310.4 kJ mol^{-1}, as shown in Fig. 6 using a pink line. This result suggests that the isomerization reaction of *cis*-COOH into HCOO is less favorable in comparison with the dissociation of *cis*-COOH into the coadsorbed CO and H_2O.

3.2.5. Brief summary

Fig. 6 presented the potential energy profiles of the most favorable routes for CO_2 hydrogenation to HCOO and to CO on H(Pd4). We can see that, on H(Pd4), the highest barrier and reaction energy with respect to H(R), for the formation of HCOO are 143.4 and 31.2 kJ mol^{-1}, respectively, while those for CO formation are 267.3 and −41.9 kJ mol^{-1}, respectively. As a result, HCOO formation is more favorable kinetically, whereas CO formation is preferred thermodynamically. However, the highest barrier of CO formation is far larger than that of HCOO formation, which means that HCOO species is the dominant product of the initial steps of CO_2 hydrogenation on H(Pd4). Since HCOO is the key intermediate to form methanol in CO_2 hydrogenation, CO_2 hydrogenation on H(Pd4) can lead to the dominant product methanol. In addition, the migration of H_c adatom from the supported Pd4 cluster to the adsorbed CO_2 is still an essential step in CO_2 hydrogenation on H(Pd4), suggesting that the hydrogen source of HCOO is the H_c atom adsorbed on the Pd cluster, but not the H_a atom of the O_wH_a group on the hydroxylated γ-Al_2O_3(1 1 0) surface.

3.3. Comparison with ideal Pd(1 1 1) surface

In order to understand the effect of the support and Pd particle size on CO_2 hydrogenation, we further investigate the CO_2 hydrogenation on an ideal $p(2 \times 2)$ Pd(1 1 1) surface, which is used to model the large Pd particle sizes. The potential energy profiles of the most favorable routes for CO_2 hydrogenation to HCOO and to CO on Pd(1 1 1) surface are shown in Fig. 7. The details of CO_2 hydrogenation to HCOO and to CO on Pd(1 1 1) surface have been presented in Supplementary materials.

We can see from Fig. 7 that the highest barrier and reaction energy for HCOO formation on Pd(1 1 1) surface with respect to CO_2 + H species in a black line are 139.9 and 30.3 kJ mol^{-1}, respectively, whereas those for the formation of CO in a red dash line are 150.2 and 66.6 kJ mol^{-1}, respectively. Our result means that the formation of CO_2 is preferable both kinetically (10.3 kJ mol^{-1}) and thermodynamically than CO formation (36.3 kJ mol^{-1}). However, we think that the differences between HCOO and CO formations thermodynamically and kinetically are small. Thus, we can conclude that the reaction of HCOO and CO formations for CO_2 hydrogenation on Pd(1 1 1) surface should be a parallel pathway, namely, both HCOO and CO are the dominate products for CO_2 hydrogenation, which means that Pd(1 1 1) surface, the large Pd particle sizes, has not shown strong selectivity and activity for CO_2 hydrogenation to HCOO or CO.

3.4. General discussion

3.4.1. The effect of hydroxylation on CO_2 hydrogenation

Fig. 8 shows a simplified potential energy diagram by only including the highest barrier for conversion of CO_2 to HCOO and CO on D(Pd4), H(Pd4) and Pd(1 1 1) surface, respectively. As shown in this figure, our results first show that on D(Pd4), the formation of CO is the dominant product of the initial steps of CO_2 hydrogenation, since CO is the product of a reverse WGS reaction and likely leads to methane, CO_2 hydrogenation on D(Pd4) likely result in the dominant product methane. Meanwhile, CO is also likely to further hydrogenate leading to methanol, which means that CO is the carbon source of CO_2 hydrogenation to methanol on D(Pd4), this result may be the reason why CO is widely used to hydrogenate to product methanol on Pd catalyst in the previous experimental studies [29,36,37,78]. On H(Pd4), the dominant product of the initial steps of CO_2 hydrogenation is HCOO, which is the key intermediate in CO_2 hydrogenation to methanol, so CO_2 hydrogenation on H(Pd4) can lead to the dominant product methanol, in which CO_2 is the carbon source for the formation of methanol. However, on Pd(1 1 1) surface, the large Pd particle sizes has not an obvious effect on the selectivity of CO_2 hydrogenation, both CO and HCOO are the dominant products of the initial steps of CO_2 hydrogenation.

On the basis of above results, we can obtain that small size Pd particles supported on γ-Al_2O_3 offer new properties for CO_2 hydrogenation different from those of bulk metal Pd, due to the presence of low coordination atoms from 9 Pd neighbors on the (1 1 1) surface to 3 neighbors for the tetramer. For example, on D(Pd4) catalyst, although Pd4 cluster supported on dry γ-Al_2O_3(1 1 0) surface significantly increase the activation barrier of CO_2 hydrogenation to HCOO in comparison with the unsupported Pd catalyst (Pd(1 1 1) surface), D(Pd4) catalyst obviously increase the difference between HCOO and CO formations thermodynamically and kinetically, indicating that D(Pd4) catalyst show strong selectivity for conversion of CO_2 hydrogenation to CO. Similarly, on H(Pd4), Pd4 cluster supported on the hydroxylated γ-Al_2O_3(1 1 0) surface significantly increase the activation barrier of CO_2 conversion to CO, however, H(Pd4) catalyst only slightly increases the activation barrier of CO_2 conversion to HCOO, suggesting that H(Pd4) catalyst show strong selectivity for CO_2 hydrogenation to HCOO. Hence, the presence and number of low-coordinated Pd active sites is of great importance to the overall activity and selectivity of CO_2 hydrogenation, which will depend on particle size and morphology. In addition, since our aim in this study is to focus on the effect of support γ-Al_2O_3 surface hydroxylation on CO_2 hydrogenation, what size of Pd particle supported on γ-Al_2O_3 is the most suitable for the selectivity and activity of CO_2 hydrogenation, this question will be considered in our future work.

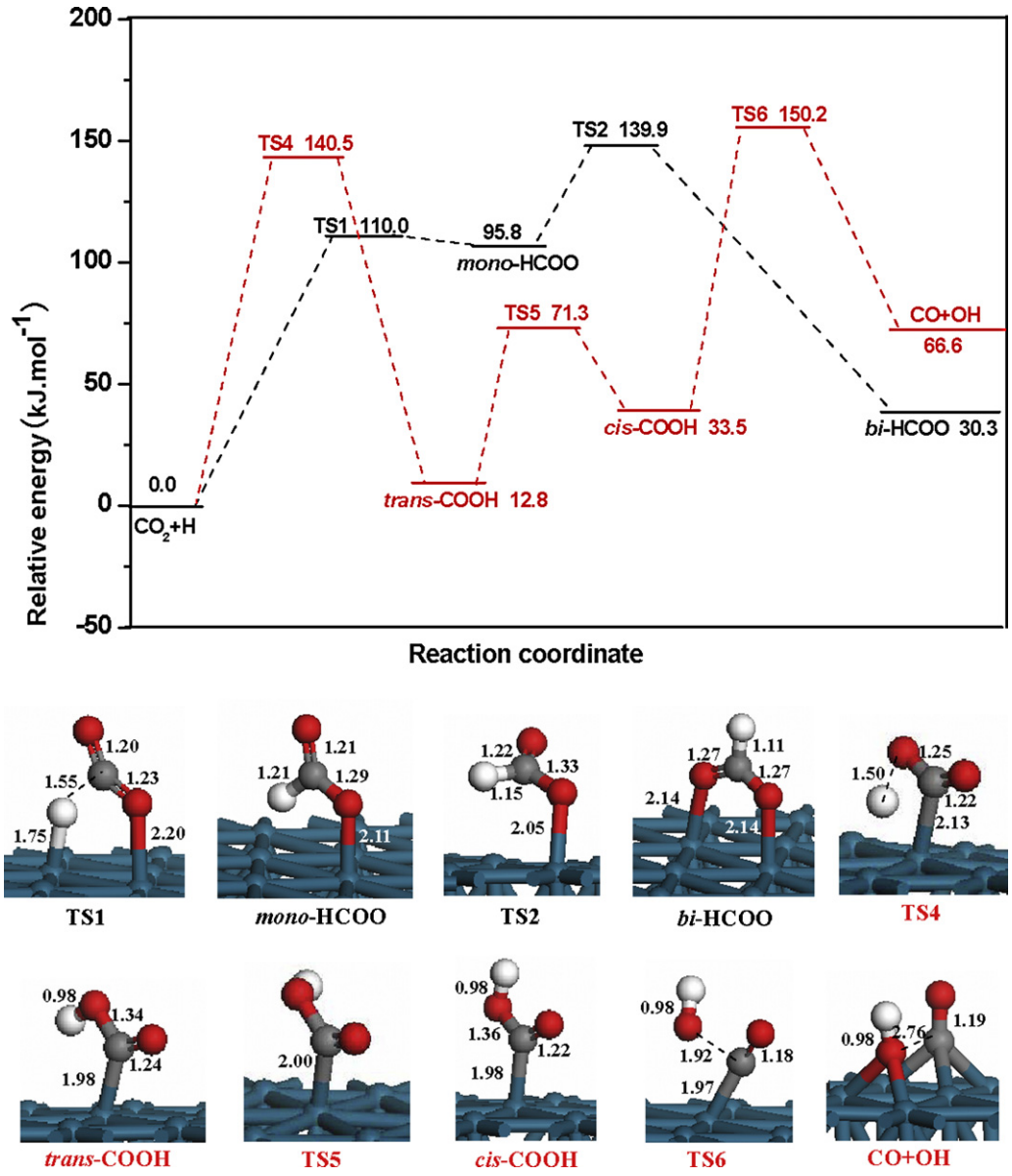

Fig. 7. Potential energy profiles of the most favorable pathway for CO_2 hydrogenation to HCOO (black line) and to CO (red line) on Pd(1 1 1) surface. Structures of the intermediates, transition states and products are also shown together with the potential energy profiles. Bond lengths are in Å. See Figs. 1 and 2 for color coding. (For interpretation of the references to color in this figure legend, the reader is referred to the web version of the article.)

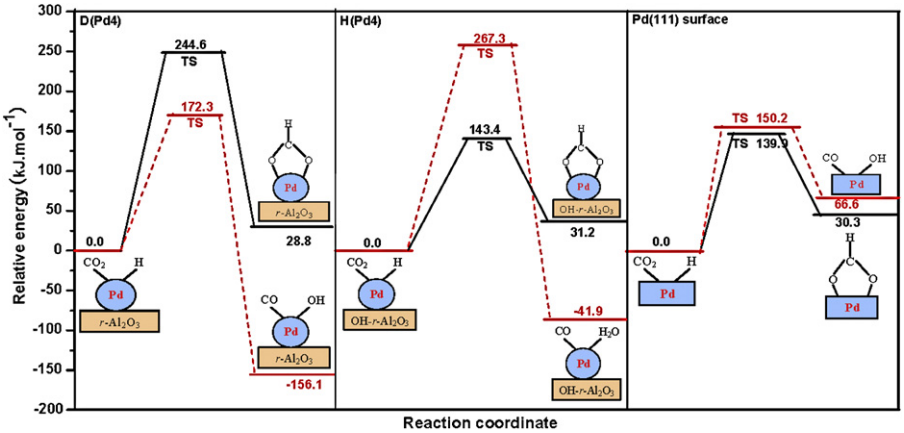

Fig. 8. Schematic potential energy diagrams of CO_2 hydrogenation to HCOO and to CO on D(Pd4), H(Pd4) and Pd(1 1 1) surface, respectively. Only transition state (TS) with the highest barrier for each path is shown.

Table 1
The hydroxylation effect on the selectivity of the initial CO_2 hydrogenation among Cu/γ-Al_2O_3, Ni/γ-Al_2O_3 and Pd/γ-Al_2O_3 catalysts.

Catalyst species	Final products	
	Dry γ-Al_2O_3	Hydroxylated γ-Al_2O_3
Cu/γ-Al_2O_3	HCOO	HCOO
Ni/γ-Al_2O_3	HCOO	CO
Pd/γ-Al_2O_3	CO	HCOO

Meanwhile, our results are in agreement with the experimental facts by Erdöhelyi and co-workers [34,35], which reported the hydrogenation of CO_2 over Pd particles supported by Al_2O_3, bonded CO and HCOO species detected by in situ IR were present on the catalyst surface during the reaction, as a result, although the size of Pd particle in above reported study may be significantly larger than that of Pd4 cluster in our study, these experimental facts still provide us a good reference, our results may contribute to a better understanding of the differences in the competing mechanisms of the reverse water gas shift and methanol synthesis reactions.

More importantly, our results demonstrate that hydroxylation of the γ-Al_2O_3 support plays an important role in determining the selectivity of CO_2 hydrogenation and carbon source of methanol formation, when CO_2 hydrogenation occurs on Pd/γ-Al_2O_3 catalyst, namely, the properties of γ-Al_2O_3 support plays a key role in changing the qualitative and quantitative trend for CO_2 hydrogenation to HCOO or CO on Pd/γ-Al_2O_3 catalyst, the properties of γ-Al_2O_3 support lead to the change of metal–support interaction, and ultimately alter the selectivity of CO_2 hydrogenation. Herein, we can conclude that the support γ-Al_2O_3 in Pd/γ-Al_2O_3 catalyst plays dual roles: one is to anchor the suitable size Pd particles on the support to improve the selectivity of CO_2 hydrogenation, and the other is to mainly provide different properties of support under given experimental conditions for CO_2 hydrogenation to alter the selectivity of CO_2 hydrogenation. Both functions are strongly dependent on the interaction of metal Pd-support γ-Al_2O_3. Therefore, we think that varying the properties of support can affect the interaction of metal–support, ultimately, alter the selectivity of CO_2 hydrogenation, which can provide a direction to the design of improved catalysts in CO_2 hydrogenation.

On the other hand, we briefly summary the hydroxylation effect on the selectivity of CO_2 hydrogenation where CO_2 hydrogenation is carried out at different active metal species among Cu/γ-Al_2O_3 [79], Ni/γ-Al_2O_3 [52] and Pd/γ-Al_2O_3 catalysts. The final products of the initial step of CO_2 hydrogenation among Cu/γ-Al_2O_3, Ni/γ-Al_2O_3 and Pd/γ-Al_2O_3 catalysts are listed in Table 1. We can see that that when different metal species are supported over γ-Al_2O_3 in CO_2 hydrogenation, the hydroxylation of the γ-Al_2O_3 support show different selectivity for CO_2 hydrogenation over every metal species, and ultimately affect the distribution of the final products. Meanwhile, we simply analyze the possible reasons for the striking distinct behaviors obtained for these three metals. In particular, the interaction of metal–support can be modified by varying the properties of support, which in turn influences the density and distribution of the active sites for adsorption and activation of CO_2 and the reaction intermediates. For instance, on Ni/γ-Al_2O_3 catalyst, the proton (Brønsted acid site) on the hydroxylated surface first involve the activation of CO_2 to form a carboxyl species, which may then lead to the preferential formation of CO + OH species. On Cu/γ-Al_2O_3 and Pd/γ-Al_2O_3 catalysts, the proton on the hydroxylated surface has not participated in the activation of CO_2, however, the hydroxylated surface facilitates the transfer of H atom adsorbed on Cu or Pd cluster and improve its interaction with CO_2, which may result in the preferential formation of HCOO species. The change of support properties alters the interaction of metal–support; ultimately, alter the selectivity of CO_2 hydrogenation.

3.4.2. The design direction of improved catalyst in CO_2 hydrogenation

It is well known that water is an unavoidable by-product in CO_2 hydrogenation under a realistic reaction condition, γ-Al_2O_3 has a greater affinity toward water, and easily form the hydroxyls on the γ-Al_2O_3, as a result, the presence of hydroxyls on γ-Al_2O_3 is inevitable [48,80]. Thus, in CO_2 hydrogenation over the metal catalysts supported on γ-Al_2O_3, HCOO should be the key intermediate, and methanol is expected to be the dominant product [81]. However, our results show that the existence of surface hydroxyls on the γ-Al_2O_3 support will weaken the interaction of metal Pd-support γ-Al_2O_3 and destabilize the catalyst, the weakness of the metal–support interaction means that the existence of surface hydroxyls can decrease the dispersion of Pd on γ-Al_2O_3 support. Erdöhelyi et al. [34] and Solymosi et al. [35] have studied the hydrogenation of CO_2 over Pd particles supported by Al_2O_3, their experimental facts show that the dispersion of Pd plays a governing role in determining the selectivity of the $H_2 + CO_2$ reaction, indicating that on highly dispersed Pd, the main product of the reaction is methane, while on low dispersed Pd methanol formation occurs. Similarly, although Pd particle in above reported study may be significantly larger than Pd4 cluster in our study, these experimental facts still provide us a good reference, our calculated results in this study show that methane is the dominant product on D(Pd4) with highly dispersed Pd, whereas methanol is the dominant product on H(Pd4) with low dispersed Pd.

These concepts can be applied to analyze previous experimental facts and help provide a design direction for the improved catalysts in CO_2 hydrogenation. For example, metal oxides such as ZnO are known to have a low affinity toward water and, therefore, are difficult to be hydroxylated [82]. Simultaneously, ZnO can improve metal dispersion [6]. Moreover, ZrO_2 has also been used as a good promoter or support to uniformly dispersed active species for the methanol synthesis catalyst because it bears high stability [83,84]. This may be the reason that ZnO or ZrO_2 has been used as a key ingredient in methanol synthesis catalysts. Therefore, on the basis of these results, we can obtain the direction for the design of the improved catalyst in the selective hydrogenation of CO_2 to methane or methanol on Pd/γ-Al_2O_3 catalysts. For methane formation, we should inhibit the hydroxylation of the γ-Al_2O_3 support by the addition of metal oxides or other components as inhibitor. Whereas, for methanol formation, we should consider two points, one is to increase the dispersion of the active species; the other is to inhibit the hydroxylation of the γ-Al_2O_3 support in a reasonable range, and these two points can be realized by the addition of metal oxides or other components as the promoter to improve its dispersion, or that as an inhibitor to prevent the hydroxylation. Generally, the processes of CO_2 conversion are regulated by many factors, including catalyst/co-catalyst, supporting oxides, promoters as well as reaction environment. Our calculated results can only provide the basis and one of the directions to the design of improved catalysts in CO_2 hydrogenation for methanol, methane and other products.

On the other hand, CO_2 is found to adsorb on Pd4/γ-Al_2O_3 negatively charged and in bent configuration, indicating a partial activation of CO_2. However, on Pd(1 1 1) surface, we observe that CO_2 interacts weakly with the Pd(1 1 1) surface, for all adsorption sites, CO_2 is far away from the surface in the optimized configurations, and the C—O bond lengths and the angle of O—C—O are close to those in the gas phase CO_2 molecule. A comparison of the results obtained for supported Pd4 cluster and Pd(1 1 1) surface (model of large Pd particle sizes) confirms that the adsorption and activation ability of CO_2 are increased for the supported Pd4 cluster. This is a consequence of the decrease of metal coordination from 9 Pd neighbors on the (1 1 1) surface to 3 neighbors for the tetramer. Pd atoms with a lower coordination number clearly develop a stronger

interaction with the adsorbate, in a manner congruent with the bond order conservation principle [43]. As a result, both the supported Pd and the support, either dry or partially hydroxylated γ-Al_2O_3, contribute to the adsorption and activation of CO_2 by donating their electronic charges to the adsorbed CO_2. Thus, we think that enhancing the adsorption and activation of CO_2 on the catalysts is also one of the possible methods, which is beneficial to the conversion of CO_2, and ultimately, the activity and selectivity.

Finally, the theoretical study with density functional theory can give us a deeper insight into the reaction mechanism of CO_2 selective hydrogenation on metal species supported on γ-Al_2O_3(M/γ-Al_2O_3) catalysts, which is relevant for a rational design of modified M/γ-Al_2O_3 systems. In our next work, the effect of a higher concentration of hydrogen atoms on Pd4 clusters, specific hydroxyl coverage of γ-Al_2O_3 surface and suitable size Pd particle supported on γ-Al_2O_3 on CO_2 selective hydrogenation will be in detail considered. The theoretical study will be a valuable tool for clarifying these questions in order to understand the further design and properties of new M/γ-Al_2O_3 systems in catalytic hydrogenation of CO_2 to methanol, methane and other products.

4. Conclusions

In this work, with the aiming of probing into the hydroxylation effect of γ-Al_2O_3 support on the selectivity in CO_2 hydrogenation on the γ-Al_2O_3-supportd metal Pd (Pd/γ-Al_2O_3) catalyst, we have studied the elementary steps of CO_2 hydrogenation leading to HCOO and CO formation on Pd/γ-Al_2O_3 catalyst by using density functional theory together with slab calculations. A tetrahedral 4-atom Pd cluster, Pd4, is supported on the dry γ-Al_2O_3(1 1 0) surface and the partially hydroxylated γ-Al_2O_3(1 1 0) surface to model the Pd/γ-Al_2O_3 catalysts: D(Pd4) and H(Pd4), respectively.

On D(Pd4), CO formation becomes more favorable both kinetically and thermodynamically. On H(Pd4), the formation of HCOO species is preferred kinetically; CO formation is more facile thermodynamically; however, the highest barrier of CO formation is far larger than that of HCOO formation, suggesting that the dominant product of the initial steps of CO_2 hydrogenation on H(Pd4) is HCOO. Our results about CO_2 hydrogenation on D(Pd4) and H(Pd4) clearly show that the hydroxylation of γ-Al_2O_3 support on Pd/γ-Al_2O_3 catalyst plays an important role in determining the selectivity of CO_2 hydrogenation and carbon source of methanol formation on Pd/γ-Al_2O_3 catalyst, suggesting that varying the properties of support can improve the selectivity of CO_2 hydrogenation, Furthermore, the migration of H adatom from the supported Pd4 cluster to adsorbed CO_2 is an essential step for CO_2 hydrogenation to HCOO and CO on Pd/γ-Al_2O_3 catalyst, and the adsorbed H atom is the hydrogen source of HCOO.

Finally, our results show that the surface hydroxyls on the γ-Al_2O_3 support will weaken the interaction of metal Pd–support γ-Al_2O_3 and destabilize the catalyst, and the weakness of the interaction between metal and support means that the surface hydroxyls can decrease the dispersion of Pd on γ-Al_2O_3 support. On the basis of this result, we can obtain the direction for the design of the improved catalyst in the selective hydrogenation of CO_2 to methanol or methane by the addition of other metal oxides or other components as the promoter to improve its dispersion, and that as an inhibitor to prevent the hydroxylation, which can provide the basis and one of the directions to the design of improved catalysts in CO_2 hydrogenation for methanol, methane and other products.

Supplementary materials

A detailed study about the adsorption structure of CO_2 and H adatom separately on D(Pd4) and H(Pd4) is first presented, then, both the details of the less favorable pathway for HCOO formation on H(Pd4) and the details of CO_2 hydrogenation to HCOO and to CO on Pd(1 1 1) surface are provided.

Acknowledgment

The authors gratefully thank the National Natural Science Foundation of China (20906066, 20976115), and the Younger Natural Science Foundation of Shanxi Province (no. 2009021015).

References

[1] J.G. Wu, M. Saito, M. Takeuchi, T. Watanabe, Applied Catalysis A-General 218 (2001) 235–240.
[2] C.S. Song, Catalysis Today 115 (2006) 2–32.
[3] L.C. Grabow, M. Mavrikakis, ACS Catalysis 1 (2011) 365–384.
[4] D.L. Chiavassa, J. Barrandeguy, A.L. Bonivardi, M.A. Baltanás, Catalysis Today 133–135 (2008) 780–786.
[5] E.E. Benson, C.P. Kubiak, A.J. Sathrum, J.M. Smieja, Chemical Society Reviews 38 (2009) 89–99.
[6] X.M. Liu, G.Q. Lu, Z.F. Yan, J. Beltramini, Industrial and Engineering Chemistry Research 42 (2003) 6518–6530.
[7] K.P. Yu, W.Y. Yu, M.C. Kuo, Y.C. Liou, S.H. Chien, Applied Catalysis B: Environmental 84 (2008) 112–118.
[8] C. Schild, A. Wokaun, R.A. Koeppel, A.J. Balker, Journal of Physical Chemistry 95 (1991) 6341–6346.
[9] A. Kiennemann, J. Idriss, J.P. Hindermann, J.C. Lavalley, A. Vallet, P. Chaumette, P. Courty, Applied Catalysis 59 (1990) 165–184.
[10] M. Bowker, R.A. Hadden, H. Houghton, J.N.K. Hyland, K.C. Waugh, Journal of Catalysis 109 (1988) 263–273.
[11] J.L. Falconer, E.A. Zagli, Journal of Catalysis 62 (1980) 280–285.
[12] A. Tahri, A. Amariglio, M. Zyad, H. Amariglio, Journal de Chimie Physique et de Physico-Chimie Biologique 90 (1993) 123–137.
[13] G.D. Weatherbee, C.H. Bartholomew, Journal of Catalysis 77 (1982) 460–472.
[14] N.M. Gupta, V.S. Kamble, V.B. Kartha, R.M. Iyer, K.R. Thampi, M. Gratzel, Journal of Catalysis 146 (1994) 173–184.
[15] A. Tahri, A. Amariglio, M. Zyad, H. Amariglio, Journal de Chimie Physique et de Physico-Chimie Biologique 90 (1993) 109–121.
[16] Y.X. Yang, J. Evans, J.A. Rodriguez, M.G. White, P. Liu, Physical Chemistry Chemical Physics 12 (2010) 9909–9917.
[17] D.W. Goodman, Accounts of Chemical Research 17 (1984) 194–200.
[18] J.R. Rostrup-Nielsen, in: J.R. Anderson, M. Boudart (Eds.), Catalysis, Science and Technology, vol. 5, Springer-Verlag, Berlin, 1983.
[19] R.D. Kelley, D.W. Goodman, in: D.A. King, D.P. Woodruff (Eds.), The Chemical Physics of Solid Surfaces and Heterogeneous Catalysis, vol. 4, Elsevier Science Publishers, Amsterdam, 1980.
[20] I.N. Remediakis, F. Abild-Pedersen, J.K. Nørskov, Journal of Physical Chemistry B 108 (2004) 14535–14540.
[21] H.H. Kung, Catalysis Reviews: Science and Engineering 22 (1980) 235–259.
[22] S.H. Ali, J.G. Goodwin Jr., Journal of Catalysis 176 (1998) 3–13.
[23] G.C. Chinchen, P.J. Denny, J.R. Jennings, M.S. Spencer, K.C. Waugh, Applied Catalysis 36 (1988) 1–65.
[24] C. Sudhakar, M.A. Vannice, Journal of Catalysis 95 (1985) 227–243.
[25] F.A.P. Cavalcanti, A.Y. Stakheev, W.M.H. Sachtler, Journal of Catalysis 134 (1992) 226–241.
[26] L. Fan, K. Fujimoto, Journal of Catalysis 150 (1994) 217–220.
[27] V. Ponec, Surface Science 272 (1992) 111–117.
[28] T. Fujitani, M. Saito, Y. Kanai, T. Watanabe, J. Nakamura, T. Uchijima, Applied Catalysis A-General 125 (1995) L199–L202.
[29] W.J. Shen, Y. Ichihashi, Y. Matsumura, Catalysis Letters 79 (2002) 125–127.
[30] S.E. Collins, M.A. Baltanás, A.L. Bonivardi, Journal of Physical Chemistry B 110 (2006) 5498–5507.
[31] S.E. Collins, M.A. Baltanás, A.L. Bonivardi, Journal of Catalysis 226 (2004) 410–421.
[32] Y.A. Ryndin, R.F. Hicks, A.T. Bell, Y.I. Yermakov, Journal of Catalysis 70 (1981) 287–297.
[33] R.F. Hicks, A.T. Bell, Journal of Catalysis 91 (1985) 104–115.
[34] A. Erdöhelyi, M. Pásztor, F. Solymosi, Journal of Catalysis 98 (1986) 166–177.
[35] F. Solymosi, A. Erdöhelyi, M. Lancz, Journal of Catalysis 95 (1985) 567–577.
[36] S. Naito, S. Aida, T. Tsunematsu, T. Miyao, Chemistry Letters 9 (1998) 941–942.
[37] S. Naito, S. Aida, T. Miyao, Studies in Surface Science and Catalysis 130 (2000) 701–706.
[38] M.A. Vannice, R.L. Garten, Industrial and Engineering Chemistry Product Research and Development 18 (1979) 186–191.
[39] M. Rothaemel, H.W. Zanthoff, M. Baerns, Catalysis Letters 28 (1994) 321–328.
[40] F. Solymosi, A. Erdohelyi, Journal of Molecular Catalysis 8 (1980) 471–474.
[41] D. Cheng, X. Zhu, Y. Ben, F. He, L. Cui, C. Liu, Catalysis Today 115 (2006) 205–210.
[42] T.J. Keskitalo, M.K. Veringa Niemelä, A.O.I. Krause, Langmuir 23 (2007) 7612–7619.
[43] M.C. Valero, P. Raybaud, P. Sautet, Journal of Catalysis 247 (2007) 339–355.
[44] D. Mei, Q. Ge, J.H. Kwak, D.H. Kim, J. Szanyi, C.H.F. Peden, Journal of Physical Chemistry C 112 (2008) 18050–18060.

[45] L. Cheng, Q. Ge, Journal of Physical Chemistry C 112 (2008) 16924–16931.
[46] O. Mekasuwandumrong, P.L. Silveston, P. Praserthdam, M. Inoue, V. Pavarajarn, W. Tanakulrungsank, Inorganic Chemistry Communications 6 (2003) 930–934.
[47] C. Meephoka, C. Chaisuk, P. Samparnpiboon, P. Praserthdam, Catalysis Communications 9 (2008) 546–550.
[48] M. Digne, P. Sautet, P. Raybaud, P. Euzen, H. Toulhoat, Journal of Catalysis 226 (2004) 54–68.
[49] Y.X. Pan, C.J. Liu, T.S. Wiltowski, Q.F. Ge, Catalysis Today 147 (2009) 68–76.
[50] S.X. Yin, T. Swift, Q.F. Ge, Catalysis Today 165 (2011) 10–18.
[51] D. Lomot, Z. Karpinski, Catalysis Letters 69 (2000) 133–138.
[52] Y.X. Pan, C.J. Liu, Q.F. Ge, Journal of Catalysis 272 (2010) 227–234.
[53] Y.X. Pan, C.J. Liu, Q.F. Ge, Langmuir 24 (2008) 12410–12419.
[54] M.C. Valero, P. Raybaud, P. Sautet, Journal of Physical Chemistry B 110 (2006) 1759–1767.
[55] M.C. Valero, P. Raybaud, P. Sautet, Physical Review B 75 (2007), 045427-1–12.
[56] M.Y. Sun, A.E. Nelson, J. Adjaye, Journal of Physical Chemistry B 110 (2006) 2310–2317.
[57] H.P. Pinto, R.M. Nieminen, S.D. Elliott, Physical Review B 70 (2004), 125402-1–11.
[58] J.H. Kwak, J.Z. Hu, D.H. Kim, J. Szanyi, C.H.F. Peden, Journal of Catalysis 251 (2007) 189–194.
[59] J.H. Kwak, J.Z. Hu, A. Lukaski, D.H. Kim, J. Szanyi, C.H.F. Peden, Journal of Physical Chemistry C 112 (2008) 9486–9492.
[60] C. Wolverton, K.C. Hass, Physical Review B 63 (2000), 24102-1–16.
[61] G. Paglia, A.L. Rohl, C.E. Buckley, J.D. Gale, Physical Review B 71 (2005), 224115-1–16.
[62] X. Krokidis, P. Raybaud, A.E. Gobichon, B. Rebours, P. Euzen, H. Toulhoat, Journal of Physical Chemistry B 105 (2001) 5121–5130.
[63] G.L. Arvizu, P. Calaminici, Journal of Chemical Physics 126 (2007) 194102–194111.
[64] G.A. Cisneros, M. Castro, D.R. Salahub, International Journal of Quantum Chemistry 75 (1999) 847–861.
[65] B. Delley, Journal of Chemical Physics 92 (1990) 508–517.
[66] B. Delley, Journal of Chemical Physics 113 (2000) 7756–7764.
[67] J.P. Perdew, K. Burke, M. Ernzerhof, Physical Review Letters 77 (1996) 3865–3868.
[68] P. Hohenberg, W. Kohn, Physical Review B 136 (1964) B864–B871.
[69] M. Dolg, U. Wedig, H. Stoll, H. Preuss, Journal of Chemical Physics 86 (1987) 866–872.
[70] A. Bergner, M. Dolg, W. Kuechle, H. Stoll, H. Preuss, Molecular Physics 80 (1993) 1431–1441.
[71] T.A. Halgren, W.N. Lipscomb, Chemical Physics Letters 49 (1977) 225–232.
[72] V. Ledentu, W. Dong, P. Sautet, Surface Science 412/413 (1998) 518–526.
[73] N. Lopez, Z. Łodziana, F. Illas, M. Salmeron, Physical Review Letters 93 (14) (2004), 146103-1–4.
[74] A.C. Luntz, J.K. Brown, M.D. Williams, Journal of Chemical Physics 93 (1990) 5240–5246.
[75] K.D. Rendulic, A. Winkler, Surface Science 299/300 (1994) 261–276.
[76] C.M.Y. Yue, K.H. Lim, Catalysis Letters 128 (2009) 221–226.
[77] S.D. Zhou, C. Qian, X.Z. Chen, Catalysis Letters 141 (2011) 726–734.
[78] P.J. Berlowitz, D.W. Goodman, Journal of Catalysis 108 (1987) 364–368.
[79] R.G. Zhang, B.J. Wang, H.Y. Liu, L.X. Ling, Journal of Physical Chemistry C 115 (2011) 19811–19818.
[80] J.A. Rodriguez, J. Evans, J. Graciani, J.B. Park, P. Liu, J. Hrbek, J.F. Sanz, Journal of Physical Chemistry C 113 (2009) 7364–7370.
[81] A.Y. Rozovskii, G.I. Lin, Topics in Catalysis 22 (2003) 137–150.
[82] A. Wander, N.M. Harrison, Journal of Chemical Physics 115 (2001) 2312–2316.
[83] C. Su, J. Li, D. He, Z. Cheng, Q. Zhu, Applied Catalysis A-General 202 (2000) 81–89.
[84] M.S. Wong, D.M. Antonelli, J.Y. Ying, Nanostructured Materials 9 (1997) 165–168.